Neurobiology of Aging 131 (2023) 196–208

Contents lists available at ScienceDirect

Neurobiology of Aging

journal homepage: www.elsevier.com/locate/neuaging.org

Grey matter volume and CSF biomarkers predict neuropsychological subtypes of MCI

Jeremy Lefort-Besnard [a], Mikael Naveau [b], Nicolas Delcroix [b], Leslie Marion Decker [a,c,*,1], Fabien Cignetti [d,**,1], for the Alzheimer's Disease Neuroimaging Initiative [2]

[a] Normandie Univ, UNICAEN, INSERM, COMETE, Caen, France
[b] Normandie Univ, UNICAEN, CNRS, CEA, INSERM, GIP Cyceron, Caen, France
[c] Normandie Univ, UNICAEN, CIREVE, Caen, France
[d] Univ. Grenoble Alpes, CNRS, VetAgro Sup, Grenoble INP, TIMC, Grenoble, France

ARTICLE INFO

Article history:
Received 6 February 2023
Revised 5 July 2023
Accepted 6 July 2023
Available online 12 July 2023

Keywords:
MCI subtypes
Neuropsychological profile
Grey matter
CSF biomarker
Alzheimer's disease neuroimaging initiative (ADNI)
Machine learning

ABSTRACT

There is increasing evidence of different subtypes of individuals with mild cognitive impairment (MCI). An important line of research is whether neuropsychologically-defined subtypes have distinct patterns of neurodegeneration and cerebrospinal fluid (CSF) biomarker composition. In our study, we demonstrated that MCI participants of the ADNI database (N = 640) can be discriminated into 3 coherent neuropsychological subgroups. Our clustering approach revealed amnestic MCI, mixed MCI, and cluster-derived normal subgroups. Furthermore, classification modeling revealed that specific predictive features can be used to differentiate amnestic and mixed MCI from cognitively normal (CN) controls: CSF $A\beta_{142}$ concentration for the former and CSF $A\beta_{1-42}$ concentration, tau concentration as well as grey matter atrophy (especially in the temporal and occipital lobes) for the latter. In contrast, participants from the cluster-derived normal subgroup exhibited an identical profile to CN controls in terms of cognitive performance, brain structure, and CSF biomarker levels. Our comprehensive data analytics strategy provides further evidence that multimodal neuropsychological subtyping is both clinically and neurobiologically meaningful.

1. Introduction

Mild cognitive impairment (MCI) is considered a transitional stage between normal aging and Alzheimer's disease (AD). There is evidence that around 10%–15% of MCI patients progress to AD each year, compared to 1%–2% in the healthy older adult population (Alzheimer's Association, 2019; Anderson, 2019). However, there is considerable heterogeneity among the MCI-diagnosed individuals, and not all of them are at risk for developing AD dementia later in life. Some patients develop non-AD dementia or other neuropsychiatric diseases (Slot et al., 2019). Others remain stable with respect to neuropsychological performance (Overton et al., 2019) or

Abbreviations: $A\beta_{1-42}$, 42 amino acid form of amyloid β peptide; AD, Alzheimer's disease; ADAS-Cog, Alzheimer's Disease Assessment Scale–Cognitive Subscale; ADNI, Alzheimer's disease neuroimaging initiative; API, application programming interface; A/T/N, amyloid, tau, neurodegeneration; CDR, clinical dementia rate; CN, cognitively normal; CDR, clinical dementia rating; CSF, cerebrospinal fluid; DSM, diagnostic and statistical manual of mental disorders; FAQ, functional activities questionnaire; FoV, field of view; FWHM, full width at half maximum; GDS, geriatric depression scale; ICBM, international consortium for brain mapping; LATE, limbic-predominant age-related TDP-43 encephalopathy; MCI, mild cognitive impairment; MMSE, Mini-Mental State Examination; MPRAGE, magnetization-prepared rapid gradient echo; MRI, magnetic resonance imaging; OvR, one-versus-rest; PCA, principal component analysis; p-tau, phosphorylated tau at threonine 181; TDP-43, transactive response DNA binding protein of 43 kDa; T-tau, total tau; TR, repetition time; TE, echo time; RAVLT, Rey Auditory Verbal Learning Test; ROI, region of interest; RR, risk ratio; SD, standard deviation; SPM, statistical parametric mapping; TMT, trial making test; VFT, verbal fluency test; WMS-R, Wechsler memory scale-revised

* Corresponding author at: UMR-S 1075, INSERM/Université de Caen Normandie, COMETE (Mobilités : Vieillissement, Pathologie, Santé), Pôle des Formations et de Recherche en Santé, 2 rue des Rochambelles, CS 14032, Caen Cedex 5, France.
** Corresponding author at: UMR 5525, CNRS/Université Grenoble Alpes, TIMC (Recherche Translationnelle et Innovation en Médecine et Complexité), Bâtiment Jean Roget, Faculté de Médecine et Pharmacie, Place du Commandant Nal, 38700 La Tronche, France.
E-mail addresses: leslie.decker@unicaen.fr (L.M. Decker), fabien.cignetti@univ-grenoble-alpes.fr (F. Cignetti).

[1] These authors contributed equally to this work.

[2] Data used in preparation of this article were obtained from the Alzheimer's disease neuroimaging initiative (ADNI) database (adni.loni.usc.edu). As such, the investigators within the ADNI contributed to the design and implementation of ADNI and/or provided data but did not participate in analysis or writing of this report. A complete listing of ADNI investigators can be found at: http://adni.loni.usc.edu/wp-content/uploads/how_to_apply/ADNI_Acknowledgement_List.pdf

0197-4580/
https://doi.org/10.1016/j.neurobiolaging.2023.07.006

even revert to normal cognitive functioning (Thomas et al., 2019a). There is also a high rate of misdiagnosis using conventional diagnostic criteria based on the DSM-5, with many "false-positive" MCI cases (Edmonds et al., 2019). This heterogeneity of MCI has led the researchers to place great emphasis on subtyping or risk stratification of MCI patients to identify those at increased risk of developing AD and who constitute the optimal target population for therapeutic interventions (Dams-O'Connor et al., 2021; Winblad et al., 2016).

A common subtyping approach is to classify MCI individuals based on their neuropsychological test scores. Early on, MCI participants were staged into early and late MCI based on their level of impairment on one memory measure, with the latter being more impaired than the former. This "classical criteria" approach can be seen in the North American Alzheimer's Disease Neuroimaging Initiative (ADNI) and in other samples (e.g., Jessen et al., 2014). This approach has proven to be useful for staging MCI severity by demonstrating a higher risk of conversion to AD in individuals with late MCI compared to those with early MCI. However, there are also a number of limits to this approach, including the unreliability of using a single neuropsychological test score to form subgroups, leading to false-positive MCI cases (Edmonds et al., 2019; Thomas et al., 2019b), as well as the low sensitivity for detecting non-amnestic forms of MCI (Jak et al., 2009). Researchers then developed "comprehensive criteria" from which multiple subtypes of MCI were identified based on performance on several tests covering a number of cognitive domains (e.g., Bondi et al., 2014; Jak et al., 2009). They consistently revealed an amnestic subtype (impaired memory), a language or dysnomic subtype (impaired language), and a mixed subtype (impaired memory, executive function, attention, verbal fluency, and visuospatial function). It should be noted that, in some studies, the dysexecutive subtype is distinguished from the mixed subtype, with memory being affected only in the latter one; while, in other studies, the mixed subtype is alternately labelled "dysexecutive" or "mixed" depending on the authors, even when referring to a subgroup with substantial impairment in overall cognitive performance, including memory. In the present study, this specific group will be referred to as "mixed MCI". Interestingly, the mixed MCI subtype has been repeatedly reported to have a higher rate of progression to AD dementia than the other subtypes. More recently, this finding has been consolidated by studies that empirically derived the exact same subtypes (i.e., amnestic and mixed) using cluster analysis performed on neuropsychological test data (Blanken et al., 2020; Edmonds et al., 2016; Machulda et al., 2019).

Several studies further characterized the above neuropsychologically-defined MCI subtypes in terms of their underlying A/T/N biomarkers, namely cerebrospinal fluid (CSF) beta-amyloid deposition ("A"), pathological tau ("T"), and neurodegeneration ("N"), as assessed from structural MRI. The objective of using the A/T/N framework for AD research (Jack et al., 2016) was to better understand the potential etiological distinctions underlying the MCI subtypes. Overall, patterns of grey matter atrophy among the MCI subtypes were found to correspond to their profiles of cognitive impairment. Amnestic MCI individuals were reported to have smaller hippocampi (He et al., 2009). Medial temporal lobe thinning was found in both the amnestic and dysnomic subtypes (Edmonds et al., 2016; Whitwell et al., 2007). Lateral temporal lobe atrophy was also found in the dysnomic subtype. A widespread pattern of grey matter atrophy spanning parietal, temporal, and frontal regions was reported in the mixed MCI subtype (Dickerson and Wolk, 2011; Edmonds et al., 2016). Regarding CSF biomarker levels (i.e., p-tau and $A\beta_{1-42}$), the mixed subtype showed a greater proportion of individuals with positive CSF AD biomarkers than the dysnomic and amnestic subtypes (Edmonds et al., 2015a). In sum, these results tend to support the idea that MCI subtypes are rather distinct in terms of their biological and cerebral injury biomarkers.

A recent study by Kwak and colleagues (2021) addressed the opposite question as to whether heterogeneity in brain atrophy patterns of MCI individuals could allow the identification of biologically and clinically meaningful subgroups. They reported one MCI subgroup in which the pattern of brain atrophy resembled that of AD patients (MCI-AD) and another MCI subgroup in which grey matter was similar to that of healthy individuals (MCI-CN). The rate of progression to AD for the MCI-AD subgroup was higher than for the MCI-CN. In terms of biological features, they reported marked differences between MCI-AD and MCI-CN subgroups, including especially more elevated tau and beta-amyloid burden in MCI-AD compared to MCI-CN. On the other hand, they found only a limited degree of overlap between these 2 MRI-derived (atrophy-centered) subgroups and those empirically derived from neuropsychological test scores, including the amnestic, dysnomic and mixed ones. Thus, whether or not neuropsychological profiles of MCI patients correspond to real distinct biological subtypes is still an open question.

In the present study, we pursue the question of the correspondence between MCI subtypes derived from neuropsychological assessment and their underlying patterns of neurodegeneration and CSF biomarker composition. For this purpose, using the ADNI data (640 MCI and 326 cognitively normal (CN) controls), we investigated the accuracy with which brain (i.e. grey matter) atrophy, on the one hand, and CSF beta-amyloid and tau levels, on the other hand, can predict neuropsychological subtypes of MCI. If predictive models derived from A/T/N biomarkers perform well in classifying neuropsychological profiles of MCI, then such findings will provide compelling evidence of concordance between neuropsychological and neurobiological subtypes. More broadly, the study will provide valuable information about the neuropsychological and neurobiological fingerprintings of MCI, and, by extension, about the need (or not) to profile patients on the basis of multi-modal assessments.

2. Methods

2.1. Participants

Data used in the preparation of this article were obtained from the ADNI database (adni.loni.usc.edu). The ADNI was launched in 2003 as a public-private partnership, led by Principal Investigator Michael W. Weiner, MD. The primary goal of ADNI has been to test whether serial magnetic resonance imaging (MRI), positron emission tomography, other biological markers, and clinical and neuropsychological assessment can be combined to measure the progression of MCI and early AD. Written informed consent was obtained from all participants or authorized representatives participating in the study. For more information, including criteria for eligibility, see http://www.adni-info.org. To be included in this work, each participant must have a status of MCI or cognitively normal (CN). CN participants showed no signs of depression, mild cognitive impairment, or dementia. ADNI criteria for MCI were: (1) subjective memory concern as reported by the participant, their study-partner or clinician, (2) abnormal memory function documented by scoring within education-adjusted ranges on delayed free recall of story A from the WMS-R Logical Memory II subtest, (3) Mini–Mental State Examination score between 24 and 30, (4) global Clinical Dementia Rating score of 0.5, with a Memory Box score of at least 0.5, and (5) general cognition and functional performance sufficiently preserved so that a diagnosis of AD could not be made. Included participants must also have a usable T1 scan (i.e., the image successfully passed preprocessing steps as well as visual quality assessment), usable CSF biomarker levels (no missing or not-a-number quantity), as well as a usable score on each questionnaire used in our study (no missing or not-a-number score). A total of 966 participants met these

Table 1
Information about the included ADNI participants

Diagnosis	N total	N male	N female	Age mean (SD)	N ADNI 1	N ADNI 2
MCI	640	376	264	73.42(7.66)	374	266
CN	326	162	164	75.15(5.57)	211	115

Sex and age were heterogeneous across groups, $X^2(8, N = 966) = 23.67$, $p < 0.01$, and, $F(3, 962) = 16.74$, $p < 0.001$, respectively. These variables were treated as confounding variables in the manuscript analyses.
Key: ADNI, Alzheimer's disease neuroimaging initiative; CN, cognitively normal; MCI, mild cognitive impairment.

conditions and were therefore included in our study. See Table 1 for more information.

2.2. Neuropsychological assessment

All MCI participants in ADNI underwent a neuropsychological assessment at baseline (visit at 1 month from the screening in the ADNI protocol). The ADNI database provided the raw results of this assessment. For our study, we selected a list of neuropsychological tests according to 2 criteria: (1) the test scores must not be missing and be a valid value, and (2) the test scores must have been used in previous studies using clustering (Edmonds et al., 2019; Park et al., 2012) in order to allow comparison of results. Neuropsychological test scores meeting these 2 criteria were included in our analysis. These tests included 3 measures of language: Animal Fluency Test, Boston Naming Test, the item Naming Objects and Fingers of the Alzheimer's Disease Assessment Scale-Cognitive Subscale (ADAS-Cog) (Rosen et al., 1984), 2 measures of executive function: Trial Making Test: score A and score B minus A, 2 measures of visuo-spatial ability: Constructional Praxis Task and Ideational Praxis Task of the ADAS-Cog, and 7 measures of memory: Word Recognition Task of the ADAS-Cog, Logical Memory II (Chelune et al., 1990), and short delayed recall, long delayed recall, recognition, learning and forgetting items of the Rey Auditory Verbal Learning Test (Rey, 1958). Neuropsychological test scores, for which a lower score represents better performance, were multiplied by minus one, so that a higher score represents better performance. All scores were then transformed into z-scores by mean centering and unit-variance scaling.

2.3. Image acquisition

Processing: The structural brain image was acquired for all participants (n = 966) with an anatomical 3D T1-weighted MPRAGE sequence. The sequence specifications of ADNI 1 session were TR = 3000 ms, TE = 3.6 ms, FoV = 192 × 192 mm^2, flip angle = 8°, voxel resolution = 1.3 × 1.3 × 1.3 mm^3, and for ADNI 2 session TR = 2300 ms, TE = 3 ms, FoV = 256 × 256 mm^2, flip angle = 9°, voxel resolution = 1 × 1 × 1 mm^3. The brain tissue was segmented into grey matter, white matter, and cerebrospinal fluid. Structural MRI data were preprocessed using SPM12 (https://www.fil.ion.ucl.ac.uk/spm/software/spm12/) toolbox implemented in Matlab 2022a (MathWorks, Inc., Natick, MA) to derive voxel-wise grey matter volumes for each participant. Standard settings of SPM12 were used for the preprocessing steps (Diffeomorphic Anatomic Registration Through Exponentiated Linear normalization to the ICBM-152 template, affine and non-linear spatial normalization). The images were segmented into grey matter, white matter, and cerebrospinal fluid, and modulated with Jacobian determinants. Finally, the modulated grey matter images were smoothed with an 8-mm isotropic FWHM Gaussian kernel. Volume extraction: Using the probabilistic Harvard-Oxford Cortical Structural lateralized atlas (RRID:SCR_001476) available from Scikit-learn (Pedregosa et al., 2011, using the argument "cort-maxprob-thr25-2mm"), quantitative measures of grey matter volume were extracted within the 96 macroscopic brain structures labeled in this atlas in every participant. For the extraction of relevant signal from the structural brain data, the total of 96 regions served as topographic masks to sum the volume information across the voxels belonging to a given region. All region-wise structural grey matter volumes were transformed into z-scores by mean centering and unit-variance scaling. Variance explained by total intracranial volume, age and sex were regressed out based on a glm approach (Friston et al., 1994). We also implemented the Combat harmonization method to robustly adjust data for site effects (Fortin et al., 2016, Johnson et al., 2007).

2.4. Collection of cerebrospinal fluid (CSF) biomarkers

The ADNI database provided the raw CSF levels of beta-amyloid plaques ($Aß_{1-42}$), total tau (t-tau), and tau phosphorylated at threonine 181 (p-tau). In this work, these 3 biomarker levels were recorded for each included participant. They were selected according to the A/T/N framework, which was proposed to differentially assess the likelihood of progression to AD dementia at the MCI stage. "A" refers to beta-amyloid deposition ($Aβ_{1-42}$), "T" refers to pathological tau, and "N" to neurodegeneration (Jack et al., 2016). More details of the CSF collection and measurements in the ADNI can be found in Shaw and colleagues (2009). All biomarkers were transformed into z-scores by mean centering and unit-variance scaling.

2.5. Identifying hidden group structure: hierarchical clustering

We applied a hierarchical clustering algorithm (agglomerative) to automatically partition patient neuropsychological profiles into homogeneous groups using the standardized (z-scored) neuropsychological scores from all MCI participants (n = 640). Hierarchical clustering is a general family of clustering algorithms that build nested clusters by merging or splitting them successively (Kärkkäinen et al. 2020). This hierarchy of clusters is represented as a tree (or dendrogram, see Fig. 1). The root of the tree is the unique cluster that gathers all individuals, while the leaves are clusters with only one individual. Here, agglomerative clustering was performed using a bottom-up approach: each observation starts in its own cluster, and clusters are successively merged together. The metric used for the merge strategy was the sum of squared differences within all clusters (Ward's method), which here was minimized. This is a variance minimization approach and, in this sense, is similar to the objective k-means function, but tackled with an agglomerative hierarchical approach. In contrast to previous approach, agglomerative clustering is a method identifying one-to-many mappings (Bzdok and Yeo, 2017): each patient is a member of exactly one group. We used "NbClust"(Charrad et al., 2014), an established R package that simultaneously applied 30 cluster validity metrics. This approach provided complementary indications on the number of groups most supported by the patient data. That is, several clustering schemes were evaluated while varying the number of clusters, to help determining the most appropriate number of clusters for our dataset. These metrics included, for example, the Duda index, the C-index, and the Gamma index. Please, see the reference above for the

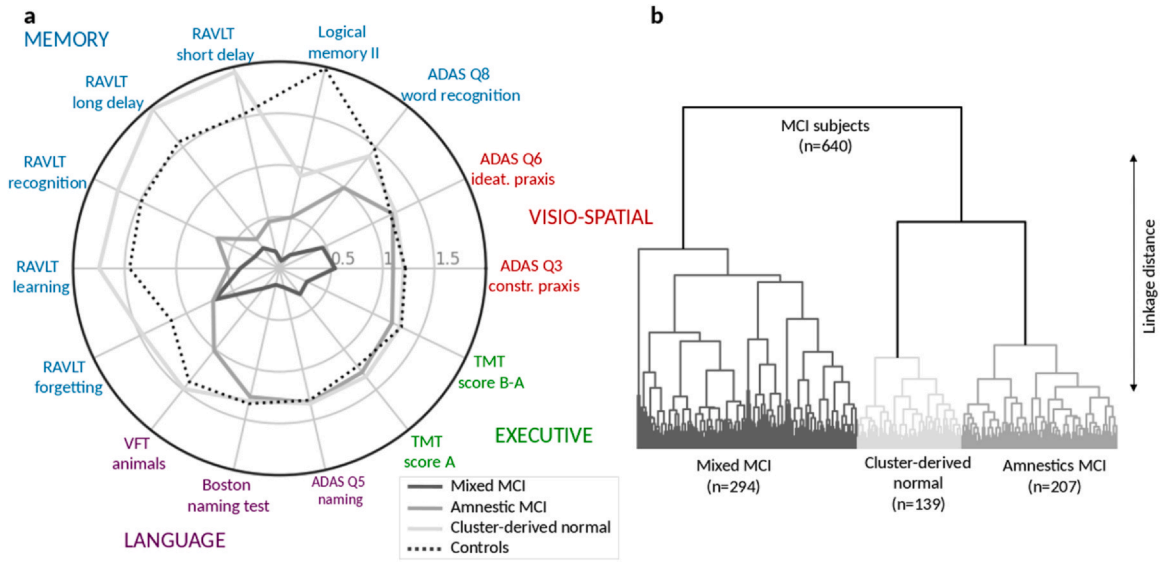

Fig. 1. Automatic extraction of 3 MCI clusters. Three subgroups were extracted from a cohort of 640 MCI patients. Polar plot (A) shows the z-score for each neuropsychological test included in the clustering procedure. The grey lines represent each extracted cluster (from darker to lighter: *mixed MCI*, *amnestic MCI*, and *cluster-derived normal*) while the dotted black line represents the z-score of cognitively normal (CN) controls. A higher score represents a greater performance. Dendrogram (B) shows the best clustering scheme, 3 subgroups according to 30 metrics, extracted from a hierarchical clustering based on a cohort of 640 MCI participants. In sum, among participants diagnosed with MCI, we could extract 3 specific subtypes, the *mixed MCI* subtype scoring low on all tests, the *amnestic MCI* subtype, scoring low on tests assessing memory, and the *cluster-derived normal* subtype, scoring mostly like CN controls except for the *logical memory II*. Abbreviation: MCI, mild cognitive impairment.

full list of metrics. Among the 30 metrics and according to the majority rule, the best number of clusters was 3 (see Supplementary Table 1). Therefore, 3 groups of patients with distinct neuropsychological profiles were automatically extracted as it provided a useful fit to our clinical sample.

2.6. Risk ratio of developing Alzheimer's disease

ADNI participants were followed and reassessed over time to track the diagnosis change. We thus scanned the recorded diagnoses and kept track of individuals who were eventually diagnosed with AD. We then used this information to compute the risk ratio (RR) in order to assess the risk of developing AD in each extracted MCI subgroup compared to CN controls. RR was defined as: RR = Cle/Clu, where Cle is the cumulative incidence in the exposed group (i.e., each MCI subgroup), and Clu is the cumulative incidence in the unexposed group (i.e., the control group).

2.7. Machine learning prediction of cluster membership from structural brain measures

The relative importance of grey matter volumes to predict membership in each MCI cluster versus CN controls was analyzed capitalizing on a pattern-learning algorithm L2-penalized logistic regression (Hastie et al., 2009). Unlike the common logistic regression, the L2-penalized logistic regression variant has an additional constraint used to reduce the chances of overfitting, which can render the models' prediction of future observation unreliable. The L2-penalized logistic regression estimated the separating hyperplane (i.e., a linear function) yielding out-of-sample accuracies for distinguishing between MCI patients of each cluster and CN controls. Model-fit and accuracy estimation were carried out as a 5-fold cross-validation procedure. Class imbalance, if present, was handled by changing the class-weight of the scikit-learn logistic regression API. The "balanced" mode uses the class membership to automatically adjust weights inversely proportional to class frequencies. The outcome to be predicted was defined by being healthy (0) or being an MCI patient from one of the 3 extracted clusters (1). In other words, 3 models were adjusted using grey matter volumes as input with a first model predicting cluster-derived normal versus CN controls, a second model predicting amnestic MCI versus CN controls, and a third one predicting mixed MCI versus CN controls. This way of engineering transformed a 4-class problem into 3 2-class problems. In sum, this quantitative investigation detected whether grey matter volumes would be predictive of cluster belonging. As a supplementary analysis, the relative importance of grey matter volumes to predict membership of MCI clusters was analyzed leveraging the one-versus-rest (OvR) L2-penalized logistic regression (Pedregosa et al., 2011). Unlike the first sets of analyses, the binary case was extended to a 3-classes problem (i.e., the 3 extracted MCI clusters). That is, instead of distinguishing between CN controls and a MCI cluster, the model will estimate the decision surface yielding out-of-sample accuracies for distinguishing between the 3 MCI subgroups. Similar settings as for the previous analysis were chosen.

2.8. Machine learning prediction of cluster membership from CSF biomarker measures

In order to allow for results comparison, the same algorithm was used in the previous setting and this one. This time, the L2-penalized logistic regression used 3 CSF biomarker level ($A\beta_{1-42}$, t-tau and p-tau) as feature input to estimate the separating hyperplane for distinguishing between MCI patients of each cluster and CN controls. Again, we deployed a 5-fold cross-validation procedure and handled class-imbalance if present. The outcome to be predicted were exactly the same as in the previous setting. That is, being healthy (0) or being an MCI patient from 1 of the 3 extracted clusters (1). Thus, 3 models were adjusted using CSF biomarker levels as input with a first model predicting cluster-derived normal versus CN controls, a second model predicting amnestic MCI versus CN controls, and a third one predicting mixed MCI versus CN controls. In sum, this

Table 2
Information about the MCI subgroups

Group	N total	N male	N female	Age M (SD)	N ADNI 1	N ADNI 2	GDS M (SD)	CDR M (SD)	FAQ M (SD)	MMSE M (SD)
Cluster-derived normal	139	64	75	70.73 (7.58)	49	90	1.83 (1.6)	0.5 (0)	1.59 (3.1)	28.53 (1.32)
Amnestic MCI	207	141	66	73.04 (7.58)	110	97	1.49 (1.32)	0.497 (0.03)	2.93 (3.6)	27.64 (1.76)
Mixed MCI	294	171	123	74.97 (7.37)	215	79	1.72 (1.37)	0.5 (0.04)	5.36 (5.3)	26.75 (1.79)

Subgroups were mapped with their scores on clinical scales to further evaluate if they reflected different stages along the course of AD or corresponded to distinct MCI phenotypes. MMSE and the FAQ scores were significantly different between MCI subgroups (respectively $F[2, 637] = 54.91$, $p < 0.001$, and $F[2, 637] = 39.50$, $p < 0.001$). Tukey's tests revealed that for both the MMSE and FAQ questionnaires, mixed MCI scored more severely (higher for the FAQ, lower for the MMSE) than amnestic MCI, which in turn scored more severely than cluster-derived normal ($p < 0.05$).
Key: AD, Alzheimer's disease; ADNI, Alzheimer's disease neuroimaging initiative; CDR, clinical dementia rating; MCI, mild cognitive impairment; MMSE, mini-mental state examination.

quantitative investigation detected if CSF biomarker levels would be predictive of cluster belonging.

As done previously, the relative importance of CSF biomarker levels to predict membership of MCI clusters was analyzed leveraging the OvR L2-penalized logistic regression (Pedregosa et al., 2011). The model will therefore estimate the decision surface yielding out-of-sample accuracies for distinguishing between the 3 MCI subgroups according to their CSF biomarker levels.

2.9. Testing for significance

Three models based on grey matter volumes and 3 other models based on CSF biomarker levels were conducted separately. Statistical significance for weights in each of the 6 final models was assessed based on (family wise error, multiple-comparison corrected) p -values derived through a rigorous non-parametric permutation approach using the model weights as the test statistic (Efron, 2010; Nichols and Holmes, 2002). Relying on minimal modeling assumptions, a valid null distribution was derived for the achieved weights resulting from the logistic regression fit. In 1000 permutation iterations, the input feature matrix (consecutively brain regions volume and CSF biomarker levels) was held constant, while the class membership (CN controls versus each cluster) underwent participant-wise random shuffling. The empirical distribution generated in this manner reflected the null hypothesis of random association between the input features and class membership across participants. The beta coefficients were recorded in each iteration. The p values were obtained given the distance between the original beta values and the mean beta values obtained during the permutation iterations.

Similarly, the significance of both the accuracies and the coefficients was assessed for the 2 OvR models (i.e., using grey matter volumes and CSF biomarker levels) using the same permutation approach.

2.10. Testing for complex relationships among features in the prediction models

We completed further analyses (1) to compare the performance of the logistic regression with other linear models, and (2) to assess whether non-linear models would reach a higher accuracy than linear models, in predicting MCI individuals (mixed MCI, or amnestic MCI, or cluster-derived normal) against CN controls. See Supplementary Methods and Results for details.

2.11. Code availability

Python was selected as the scientific computing engine. Scikit-learn (Pedregosa et al., 2011) provided efficient, unit-tested implementations of state-of-the-art statistical learning algorithms (http://scikit-learn.org). All analysis scripts of the present study are readily accessible to the reader online (https://github.com/JLefortBesnard/MCI_cluster_prediction).

3. Results

3.1. Identifying hidden group structure: hierarchical clustering

To explore distinct subgroups related to cognitive test assessment patterns among MCI patients, each patient was automatically assigned to one dominant symptom constellation based on a number of cognitive tests. This data-driven exploration revealed 3 distinct symptom clusters (see Fig. 1A and B) grouping the MCI patients: a mixed MCI subgroup (294 MCI patients) harbored low scores at almost every test (maximum 0.6 points on average), an amnestic MCI subgroup (207 MCI patients) scored low only on test assessing memory (maximum 1 point on average), and a cluster-derived normal subgroup (139 MCI patients) included MCI patients with a scoring profile virtually identical to CN controls (at least 1 point on average) except for one test, the logical memory II. More details about each subgroup's characteristics can be found in Table 2.

3.2. Repartition of MCI patients developing Alzheimer's disease

Progression to AD amounted to 28 out of 326 participants in the CN control subgroup, 14 out of 139 participants in the cluster-derived normal subgroup, 78 out of 207 participants in the amnestic MCI subgroup, and 190 out of 294 participants in the mixed MCI subgroup (see Fig. 2A and B). The occurrence of AD was different across CN controls and the 3 MCI subgroups ($X^2[8, N = 966] = 259.32$, $p < 0.001$). Bonferroni corrected post-hoc examinations revealed a larger occurrence of AD in the mixed MCI subgroup compared to the amnestic subgroup ($X^2[4, N = 533] = 67.26$, $p < 0.001$), as well as in the amnestic MCI subgroup compared to the cluster-derived normal subgroup ($X^2[4, N = 620] = 212.92$, $p < 0.001$). No difference in AD occurrence was found between CN controls and cluster-derived normal. Thus, the RR increases from cluster-derived normal (RR = 1.17) to amnestic MCI (RR = 4.39) individuals and from amnestic MCI to mixed MCI (RR = 7.52) individuals (see Fig. 2C).

3.3. Prediction of MCI subtypes versus CN controls based on grey matter volumes

We explored the hypothesis that grey matter volumes may predict MCI subgroup membership. A regularized logistic regression was used to automatically identify regions of interest (ROI) with a high discriminant value for distinguishing CN controls from each MCI subgroup (see Fig. 3A and C). Our analysis strategy revealed that only the mixed MCI subgroup was distinguishable from CN controls using grey matter volumes. The mean accuracy of the classification was 70.94% with a standard error of 1.60% (see also confusion matrix in Supplementary Fig. 1). There were 6 ROIs ($p < 0.05$) that

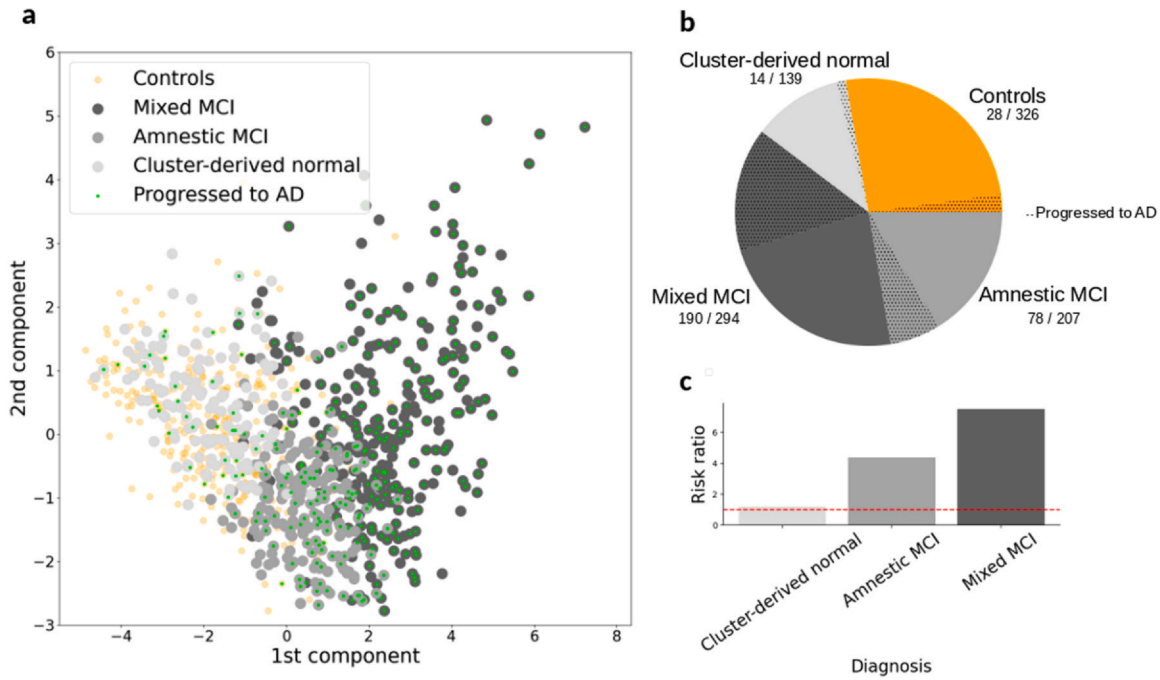

Fig. 2. Risk ratio of MCI patients developing Alzheimer's. Scatter plot (A) displays the participant first and second component of a PCA analysis on the neuropsychological tests included in our clustering analysis. Note that this PCA analysis was computed for the sake of visualization only. The green dots depict CN controls and MCI participants from the ADNI who later developed Alzheimer's disease (AD). The pie plot (B) depicts the proportion of individuals from a specific group who later developed AD (black dot). The grey bar graphs (C) display the risk ratio of developing Alzheimer's disease in each extracted subgroup compared to CN controls. The red dotted line represents a risk ratio similar to the CN control subgroup risk ratio. These results exhibit that mixed MCI patients have greatest risk to develop AD, followed by the amnestic MCI patients. Abbreviations: ADNI, American Alzheimer's disease neuroimaging initiative; MCI, mild cognitive impairment. (For interpretation of the references to color in this figure legend, the reader is referred to the Web version of this article.)

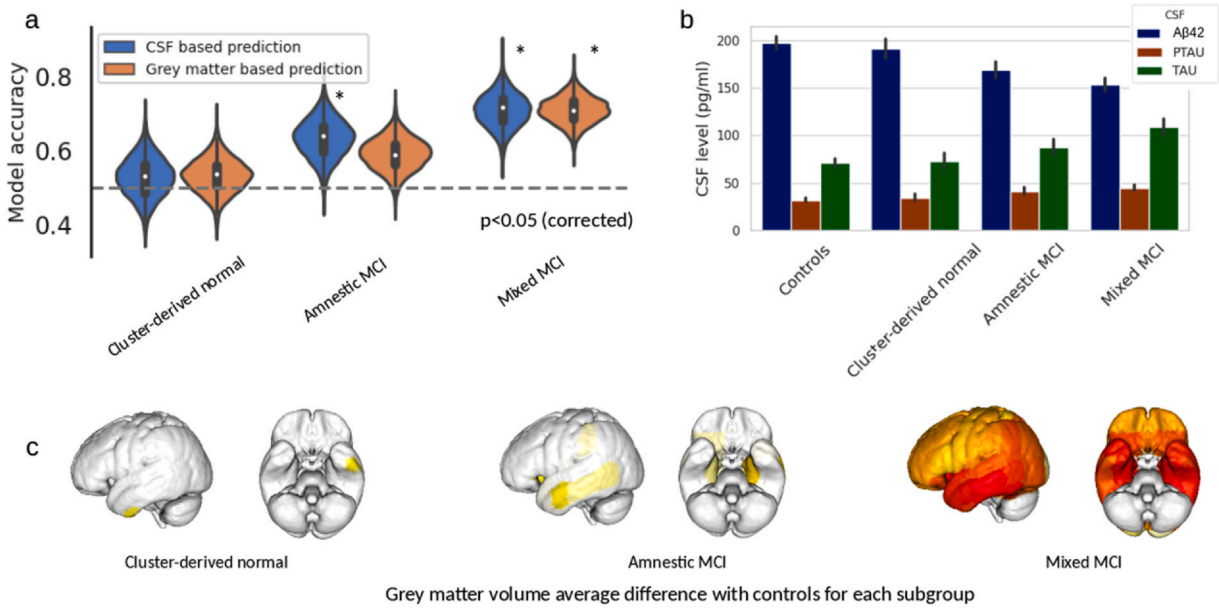

Fig. 3. Prediction of MCI clusters based on grey matter or CSF level. We explored the hypothesis that grey matter volume, on the one hand, and levels of beta-amyloid (1–42) peptide ($A\beta_{1-42}$), total tau (t-tau), and tau phosphorylated at threonine 181 (p-tau), on the other hand, may predict MCI subgroup membership. Violin plots (A) display the generalization performance (test set) of the prediction using grey matter volumes (blue) and CSF biomarker levels (orange) between CN controls and each MCI subgroup. A non-parametric test was applied to assess the significance of the accuracy (Bonferroni-corrected), that is, to evaluate if such an accuracy could be obtained by chance alone. The significant accuracies are represented with a black star. Bar graphs (B) display means (with standard deviations) CSF biomarker levels ($A\beta_{1-42}$, t-tau, and p-tau) by MCI subgroup as well as in CN controls. The brains (C) indicate the average difference of grey matter volumes between CN controls and each MCI subgroup. The redder the area, the higher the atrophy compared to CN controls. As a general observation, a better performance was achieved when dissociating mixed MCI from CN controls using grey matter volumes as well as CSF biomarker levels. The amnestic MCI subgroup was distinguishable from CN controls based on CSF biomarker levels, but not on grey matter volumes. Finally, the models could not segregate cluster-derived normal from CN controls using these modalities. Abbreviations: CSF, cerebrospinal fluid; MCI, mild cognitive impairment. (For interpretation of the references to color in this figure legend, the reader is referred to the Web version of this article.)

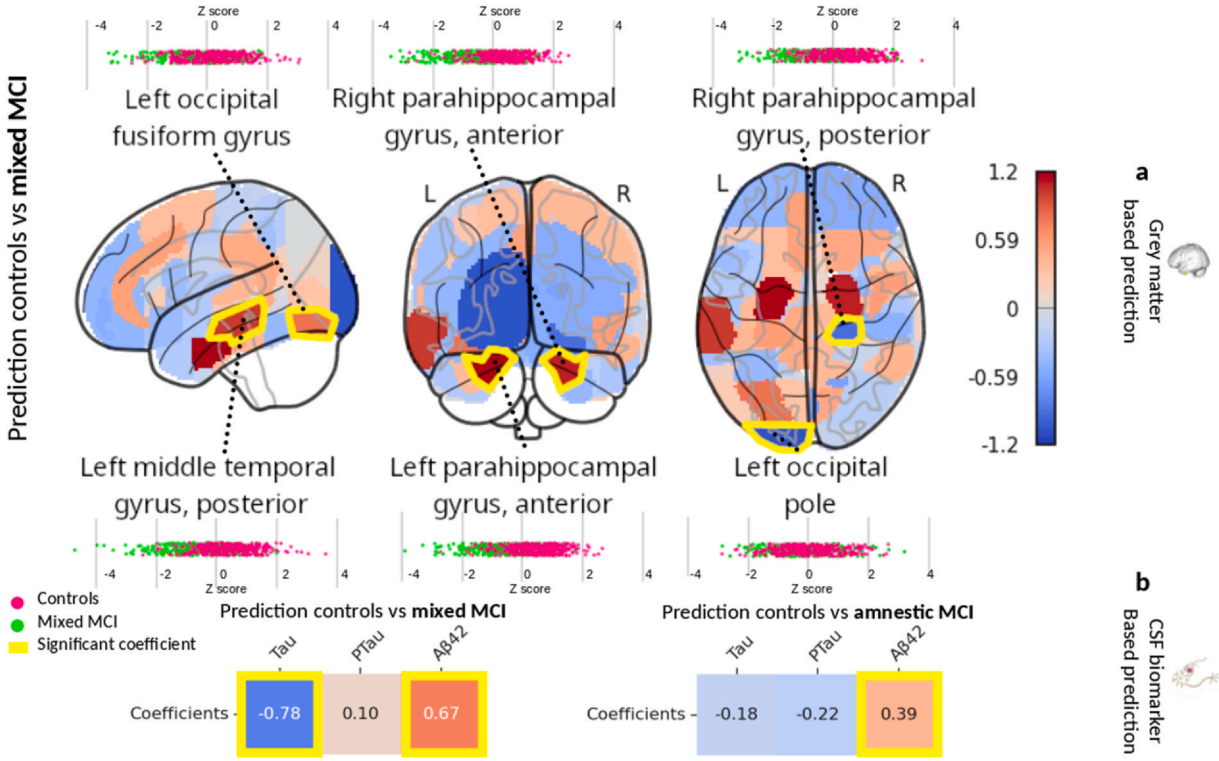

Fig. 4. Maps of coefficients for the prediction of each MCI cluster versus CN controls. Prediction of mixed MCI subgroup membership versus CN controls was assessed using grey matter volumes (A) or CSF biomarker levels (B) and using regularized logistic regression models. The colormap on each glass brain (A) depicts the final coefficient value for each ROI. A non-parametric test was computed to assess the significance of the coefficients. That is, to evaluate if a high coefficient was high only by chance or not. Significant ROIs are outlined in yellow. For each significant ROI, boxplots of the distribution of grey matter volumes per subject for CN controls (pink) and mixed MCI (light green) are displayed. The heatmap (B) displays the final coefficient value for each CSF biomarker, with significant biomarkers outlined in yellow. Regarding grey matter volumes, 6 ROIs passed the threshold (Bonferroni-corrected) and thus had a significant contribution in predicting mixed MCI versus CN controls. These ROIs are located in temporal, parahippocampal, and occipital regions, and show a larger volume in CN controls than in mixed MCI individuals. Regarding CSF, tau and Aβ42 significantly contributed to the dissociation between MCI individuals and CN controls (the 2 of them for mixed MCI and only the latter for amnestic MCI). Abbreviations: CSF, cerebrospinal fluid; MCI, mild cognitive impairment; ROI, regions of interest. (For interpretation of the references to color in this figure legend, the reader is referred to the Web version of this article.)

consistently contributed to predicting mixed MCI. These ROIs included the left occipital fusiform gyrus (weight = 0.77), the right (weight = 1.07) and left (weight = 1.17) parahippocampal gyrus anterior, the left middle posterior temporal gyrus (weight = 0.99), the left occipital pole (weight = −1.04), and the right (weight = −0.90) parahippocampal gyrus posterior (see Fig. 4A).

3.4. MCI cluster membership prediction based on grey matter volumes

As a follow-up analysis, we evaluated how grey matter volume may predict MCI subgroup membership. A regularized OvR logistic regression was used to automatically identify ROI with a high discriminant value for distinguishing each MCI subgroup (see Fig. 5, upper part). The mean accuracy of the averaged OvR models, incorporating only structural MRI data, was 43.38% (chance level = 33.33%) with a standard error of 3.90%, and was significant ($p < 0.05$). Our analysis strategy revealed 11 significant ROIs ($p < 0.05$). These ROIs included the left inferior temporal gyrus, anterior division, the left lateral occipital cortex, inferior division, the left middle temporal gyrus, posterior division, the left occipital pole, the left paracingulate gyrus, the left parahippocampal gyrus, anterior division, the right cingulate gyrus, posterior division, the right paracingulate gyrus, the right parahippocampal gyrus, anterior division, the right supracalcarine cortex, and the right temporal fusiform cortex, anterior division (see Table 3 for further details). Examination of the confusion matrix (Supplementary Fig. 2) shows that mixed MCI were better classified than the 2 other subgroups. While 3 of these ROIs were also significant in the CN controls versus mixed MCI analysis, most significant ROIs were located in similar brain areas in both analyses.

3.5. MCI cluster prediction versus CN controls based on CSF biomarker levels

We then analyzed the relative importance of the level of $A\beta_{1-42}$, t-tau, and p-tau for distinguishing CN controls from each MCI subgroup (see Fig. 3A and B). Our findings indicated a significant prediction accuracy for discriminating both the mixed MCI (70.88% +/− 2.06%) and amnestic MCI (63.35% +/− 2.32%) subgroup from CN controls. However, our model did not perform better than the chance to distinguish CN controls from the cluster-derived normal subgroup. Only the weight associated with the level of $A\beta_{1-42}$ (coefficient = 0.39) was significant in predicting amnestic MCI patients while both the level of $A\beta_{1-42}$ (coefficient = 0.67) and Tau (coefficient = −0.78) were significant in predicting mixed MCI patients (see Fig. 4B).

3.6. MCI cluster membership prediction based on CSF biomarker levels

Finally, we evaluated how CSF biomarker levels may predict MCI subgroup membership. A regularized OvR logistic regression was used to automatically identify CSF biomarkers with a high discriminant value for distinguishing each MCI subgroup (see Fig. 5, lower part). The mean accuracy of the averaged OvR models,

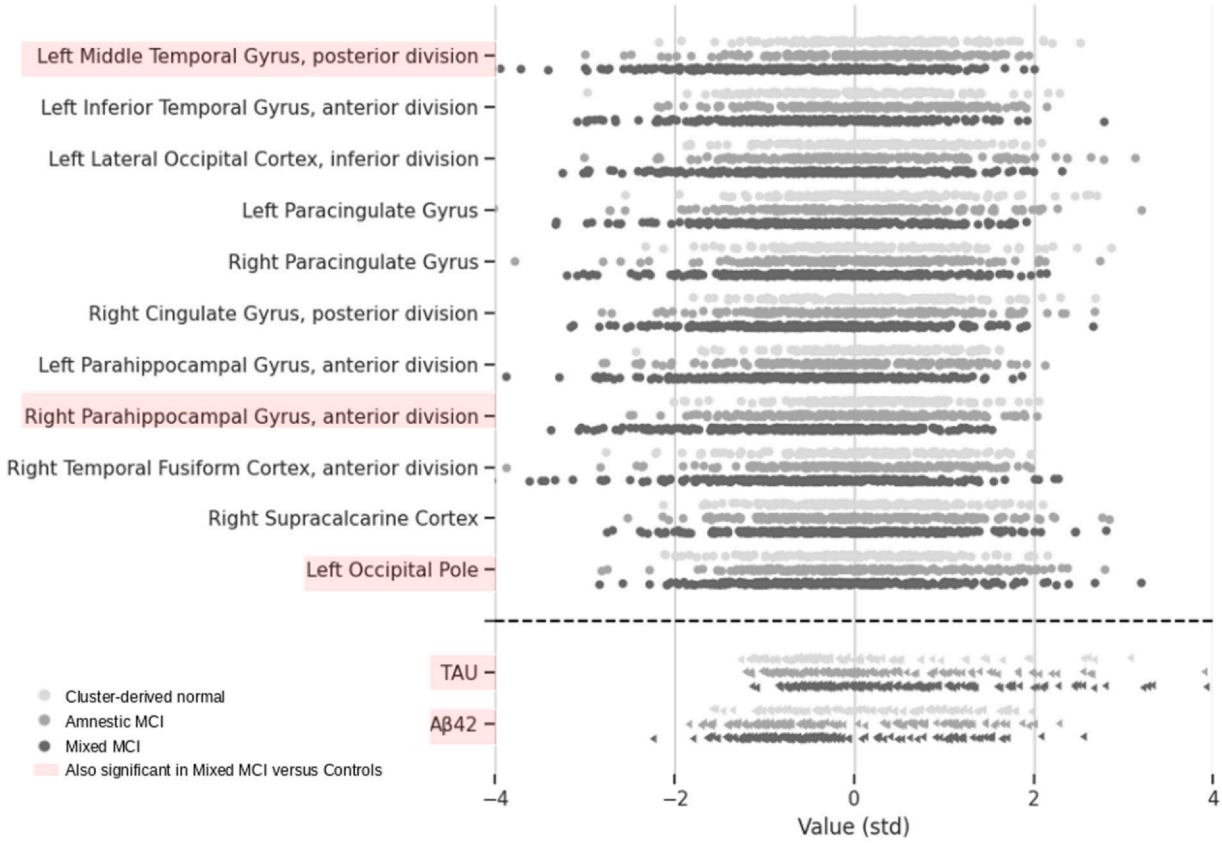

Fig. 5. Significant coefficients from multiclass classifications. Prediction of MCI subgroup membership was assessed using grey matter volume (upper part) or CSF biomarker levels (lower part) and using regularized OvR logistic regression models. Each point (shades of grey) at the top part of the figure represents the ROI volume for a specific participant in each of the 11 significant ROIs while points at the lower part represents the CSF biomarker levels for each MCI participant. Each significant ROI or CSF biomarker that was also significant in the classification of the mixed MCI subgroup versus CN controls are highlighted in pink. 11 ROIs passed the threshold and thus had a significant coefficient for distinguishing MCI subgroups on the basis of grey matter volumes alone. On the other hand, the same 2 CSF biomarkers significant for predicting mixed MCI subgroup versus CN controls were also significant in predicting MCI subgroup membership. Abbreviations: CSF, cerebrospinal fluid; MCI, mild cognitive impairment; OvR, one-versus-rest; ROI, regions of interest. (For interpretation of the references to color in this figure legend, the reader is referred to the Web version of this article.)

Table 3
Significant ROI weights for the multiclass OvR analysis

	Cluster-derived normal	Amnestic MCI	Mixed MCI
Left Middle Temporal Gyrus, posterior division		0.75	−0.84
Left Inferior Temporal Gyrus, anterior division	−0.84		
Left Lateral Occipital Cortex, inferior division	0.74		
Left Paracingulate Gyrus	0.99		−0.88
Right Paracingulate Gyrus	−1.15		
Right Cingulate Gyrus, posterior division		−0.93	
Left Parahippocampal Gyrus, anterior division	0.83		
Right Parahippocampal Gyrus, anterior division	0.77		
Right Temporal Fusiform Cortex, anterior division	−0.78		
Right Supracalcarine Cortex	−0.92		
Left Occipital Pole	−0.87		

Key: MCI, mild cognitive impairment; OvR, one-versus-rest; ROI, region of interest.

incorporating only CSF biomarker level data, was 45.89% (chance level = 33.33%) with a standard error of 4.53% and was also significant ($p < 0.05$). Our analysis strategy revealed 2 significant CSF biomarkers ($p < 0.05$), namely $A\beta_{1-42}$ and Tau levels (see Table 4 for further details). These 2 CSF biomarkers were also significant in the CN controls versus mixed MCI analysis while CSF $A\beta_{1-42}$ level was also significant in the CN controls versus amnestic MCI analysis. Examination of the confusion matrix (Supplementary Fig. 2) shows that mixed MCI and cluster derived-normal were better classified than the amnestic MCI subgroup.

4. Discussion

Our study uncovered 3 partitions of discrete neuropsychologically-based MCI profiles. The first extracted MCI profile was similar to CN controls in terms of grey matter volumes, CSF biomarker levels, neuropsychological test scores, as well as risk of developing Alzheimer's disease. The 2 other extracted MCI profiles showed regional grey matter volume reductions and abnormal CSF biomarker levels, allowing their discrimination from CN controls, and were also more at risk of developing Alzheimer's disease. These results support

Table 4
Significant CSF biomarker weights for the multiclass OvR analysis

	Cluster-derived normal	Amnestic MCI	Mixed MCI
Tau			0.47
$A\beta_{1-42}$	0.42		−0.34

Key: Aβ, beta-amyloid; CSF, cerebrospinal fluid; MCI, mild cognitive impairment; OvR, one-versus-rest.

the conclusion that MCI subtypes derived from neuropsychological test scores have relatively clear biological – grey matter volumes and CSF features – boundaries.

4.1. Subtyping patients with MCI using neuropsychological test scores

Our clustering method revealed two distinct, clinically meaningful subgroups of MCI patients: a mixed MCI profile with poor performance on memory, language, executive and visuo-spatial functions, and an amnestic MCI profile with memory being the only impaired domain. A third profile also came out, with a neuropsychological profile similar to CN controls. In general, these latent profiles are consistent with those reported in a number of previous studies that also applied clustering methods on a standardized set of neuropsychological tests measuring multiple domains of cognitive functioning (Blanken et al., 2020; Bondi et al., 2014; Edmonds et al. 2015a; Eppig et al., 2017). However, there are also studies that revealed additional profiles to the above-mentioned core MCI profiles, including dysexecutive, visuo-spatial or dysnomic profiles (Edmonds et al., 2015a, 2016; Kwak et al., 2021). Factors that can explain such variations in the profiles are the criteria used to define MCI (prior to the clustering analysis) as well as the set of neuropsychological test scores included in the cluster analysis. For instance, in addition to the amnestic, mixed, and cluster-derived normal profiles, Clark et al. (2013) also reported dysexecutive and visuo-spatial subtypes. However, in their study, inclusion as MCI was not based on the conventional diagnostic criterion (as in our study), but rather on a specific criterion that required poor performance on at least 2 measures within a cognitive domain. In addition, they used items from the Wechsler Intelligence Scale and Wechsler Memory Scale while we used items from the ADAS-cog for assessing visuospatial function. Likewise, studies that reported dysnomic MCI subtype assessed language from animal fluency and 30-item Boston Naming Test (Edmonds et al., 2015a; Kwak et al., 2021), while we further included the item Naming Objects and Fingers of the ADAS-Cog. An additional factor that may explain discrepancies between studies is the stability of the chosen clusters. We used multiple distance metrics (n = 30, through the *nbclust* R package) to assess the most stable number of clusters in our sample while a single metric is usually chosen in other studies. Accordingly, we are confident that the choice of 3 clusters was the most consistent and optimal solution to get non-overlapping homogeneous subgroups. It is noteworthy that the higher risk of Alzheimer's dementia observed in the mixed MCI subgroup compared to the amnestic MCI subgroup and the normal risk level of the cluster-derived normal subgroup provided clinical validity to this clustering scheme. From a clinical standpoint, the existence of these MCI subtypes illustrates the problem of diagnosing individuals on the basis of a single test in the memory domain, here the WMS-R Logical Memory Test in the ADNI study. First, it places individuals suffering solely from memory deficits side by side with individuals suffering from multi-domain cognitive deficits, who are at different risks of progression to dementia. Second, it leads to false positive MCI diagnoses. Accordingly, and in line with previous recommendations (eg., Edmonds et al., 2015a; Jak et al., 2009; Thomas et al., 2019b), MCI diagnosis should include a multi-domain neuropsychological assessment and avoid the "one test equals one domain" methodology.

4.2. Prediction of MCI subtypes from regional grey matter volumes

We automatically assessed the extent to which each MCI subgroup could be differentiated from CN controls based on regional grey matter volumes. Significant accuracy (71%) was obtained only for predicting the mixed MCI subgroup compared with CN controls. This finding suggests that the amnestic MCI subgroup and the cluster-derived normal subgroup have a brain structure more similar to CN controls. While the similarity of regional grey matter volumes in the cluster-derived normal MCI subtype and CN controls confirms the conclusion of previous studies drawn from cortical thickness (Blanken et al., 2019; Clark et al., 2013; Edmonds et al., 2016, 2020), that between the amnestic MCI subgroup and CN controls may appear surprising.

Edmonds et al. (2016, 2020) found cortical differences between these 2 populations (i.e., amnestic MCI and CN controls) in the medial and lateral temporal lobe regions bilaterally as well as in some parietal and frontal regions. Machulda et al. (2020) also found differences in the medial temporal regions. Sun et al. (2019) reported decreased cortical thickness in medial orbitofrontal, parahippocampal, and precuneus in amnestic MCI individuals. The discrepancy between these findings and ours is presumably due to differences in methodology. Indeed, previous research has focused on brain structure differences in an explanatory way (i.e., modeling for inference using statistical significance) whereas, in our study, we sought to find predictive patterns (i.e., modeling for prediction using cross-validation). In particular, there is evidence that successful prediction is often associated with a significant *p*-value, but not vice versa (Bzdok et al., 2020). Hence, previous brain structure impairments reported in amnestic MCI individuals may have rather poor predictive performance. Accordingly, brain structure should not be regarded as an indicator of main importance to detect amnestic MCI. This proposal is further supported by other studies, albeit with a rather small sample size (respectively 49 and 29 amnestic MCI), that used an explanatory approach and found no differences in brain structure between amnestic MCI individuals and CN controls (Xue et al., 2021; Yang et al., 2019).

Regarding mixed MCI, a total of 6 ROIs with decreased grey matter volume significantly contributed to the prediction performance. These ROIs included 2 regions from the occipital lobe, namely the left occipital fusiform gyrus and the left occipital pole, and 4 regions from the temporal lobe, including the right and left anterior parahippocampal gyrus, the right posterior parahippocampal gyrus, and the left middle posterior temporal gyrus. Note that the weights of 3 of these 6 ROIs (the left middle posterior temporal gyrus, the left anterior parahippocampal gyrus, and the left occipital pole) were systematically significant across the linear model benchmark analysis, suggesting a more robust predictive value for these 3 ROIs (see Supplementary Table 2). Hence, atrophy in temporal and occipital regions had predictive value for delineating mixed MCI individuals from CN controls. While widespread atrophy of temporal regions is a typical finding in mixed MCI (Edmonds et al., 2020; 2016; Ghosh et al., 2014; Johnson et al., 2010; Junquera Fernández et al., 2020; Kwak et al., 2021; Machulda et al., 2020.), occipital regions are usually only marginally affected in these individuals. Indeed, it is generally accepted so far that atrophy of the occipital cortex is characteristic of the later stages of Alzheimer's disease (Braak and Braak, 1991). Furthermore, impaired perfusion of the occipital lobe has been proposed as a determining marker of dementia with Lewy Bodies, but not really of Alzheimer's disease (Hanyu et al., 2006; Prosser et al., 2017). Hence, a striking and novel finding of our study is that grey matter

volume in the occipital cortex is affected as early as the MCI stage. Interestingly, our findings are in line with a recent conclusion that loss of grey matter integrity in the lateral and medial temporal lobes, as well as in the occipital lobe, is responsible for cognitive decline in vulnerable individuals experiencing the deleterious effects of elevated brain amyloid and poor vascular health (Saboo et al., 2022). Hence, atrophy of the temporal and occipital lobes may be very valuable marker of cognitively vulnerable individuals. On the other hand, the above-mentioned studies on mixed MCI reported significant grey matter loss in parietal and frontal regions, which were not found to be particularly predictively relevant in our study.

Multiclass classification further revealed that MCI and cluster-derived normal subgroups can be dissociated (43.38%, chance level = 33.33%) from each other on the single basis of regional grey matter volumes. ROIs that were most contributing to classification were mainly located in temporal, occipital, and parahippocampal regions, providing further support to the above-mentioned idea that these cortical regions are affected early during the prodromal stage of AD. Among the predictive ROIs, it is also worth mentioning the posterior division of the right cingulate gyrus, which is documented to be disrupted as early as the MCI stage (Scheff et al., 2015), and demonstrates early beta-amyloid deposition in the progression of AD (Ingala et al., 2021). The multiclass confusion matrix results showed that the mixed MCI subgroup was better predicted than the 2 other subgroups, suggesting a more distinguishable grey matter pattern. This discrepancy is in line with the previous analysis showing that only mixed MCI individuals were distinguishable from CN controls based on their grey matter volumes.

Finally, note that we emphasized our discussion on ROIs with the highest and most robust weights as automatically optimized by the model (i.e., L2-penalized logistic regression). However, it is important to keep in mind that any classifier chooses to shrink a ROI coefficient because it provides little or no additional information on top of the other ROIs. Therefore, ROIs with small weights may still be related to the outcome.

4.3. Predictive value of CSF biomarkers to distinguish MCI patients from CN controls

CSF biomarkers were useful to significantly differentiate (72% accuracy) between mixed MCI patients and CN controls. In particular, the weights associated with the concentration of $A\beta_{1-42}$ and concentration of t-tau were significant. That is, these 2 features were repeatedly informative for telling apart both groups. In patients, the concentration of $A\beta_{1-42}$ was lower while the concentration of t-tau was higher compared to CN controls. CSF biomarkers were also effective to significantly distinguish amnestic MCI from CN controls (63% accuracy). This time, only the weight associated with the concentration of $A\beta_{1-42}$ was significant, suggesting that the concentration of $A\beta_{1-42}$ was the most contributing feature for the prediction. Furthermore, classification of cluster-derived normal, amnestic MCI, and mixed MCI subgroups was significant (45.89%, chance level = 33.33%). Significant CSF biomarker level weights were those for $A\beta_{1-42}$ and t-tau, suggesting that these 2 biomarkers were again highly contributing to the classification. The multiclass confusion matrix results showed that the cluster-derived normal and the mixed MCI subgroups were more distinguishable than the amnestic MCI subgroup, which is also in line with the previous analysis. Indeed, mixed MCI individuals were more distinguishable from CN controls than amnestic MCI individuals, who in turn, were more distinguishable from CN controls than cluster-derived normal individuals. It was therefore easier for the model to tell apart the 2 most different subgroups. Overall, these results are in line with several previous studies that have examined biomarker characteristics in empirically derived subtypes of MCI and concluded that MCI patients with amnestic or executive symptoms have amyloid brain pathology and neuronal injury (Bangen et al., 2016; Edmonds et al., 2015a; 2016; 2021; Eppig et al., 2017; Thomas et al., 2019b). Indeed, low CSF $A\beta_{1-42}$ level and high CSF tau level are strong predictors of the presence of pathological beta-amyloid plaques and neurofibrillary abnormalities in the brain (Tapiola et al., 2009). An important outcome of our work is that t-tau was found to be a significantly informative feature to separate mixed MCI, but not amnestic MCI, from CN controls. Accordingly, both amnestic and mixed MCI subtypes would exhibit amyloid pathology while only the mixed subtype would have disrupted neuronal integrity. This conclusion is also supported by a clinical interpretation of the concentrations of CSF $A\beta_{1-42}$ and t-tau observed in our sample. In both subgroups, CSF $A\beta_{1-42}$ concentration was less than the cutoff of 192 pg/mL that is commonly used to identify the presence of amyloid pathology (Shaw et al., 2009). On the other hand, the cutoff of 93 pg/mL, which identifies disruption of neuronal integrity (Shaw et al., 2009), was exceeded in the mixed subgroup only. Finally, it is also important to draw attention to the fact that above and beyond the above-mentioned impaired levels of CSF $A\beta_{1-42}$ and t-tau in the MCI subgroups, both MCI subgroups were at higher risk to develop AD. This suggests a link between CSF biomarkers and conversion to AD, as pointed out in earlier studies (Hansson et al., 2006; Insel et al., 2018; Mattsson et al., 2009; Ortega et al., 2019; Park et al., 2019).

4.4. MCI subgroups as distinct MCI phenotypes or distinct stages along the course of Alzheimer's disease?

The mixed MCI subgroup was distinguished from CN controls through structural brain atrophy as well as CSF $A\beta_{1-42}$ and t-tau abnormal levels, while the amnestic MCI subgroup was separated from CN controls through CSF $A\beta_{1-42}$ abnormal level only. At the same time, mixed MCI individuals (1) were at higher risk of conversion to Alzheimer's disease, (2) converted to AD (from inclusion) over a shorter timespan (see Supplementary Fig. 3), and (3) had lower functional and cognitive abilities (as assessed from FAQ and Mini-Mental State Examination, respectively; see Table 2), than amnestic MCI individuals. Similar trends were observed between amnestic MCI individuals and CN controls, as well as between cluster-derived normal individuals and CN controls. Overall, these findings are consistent with the amyloid cascade model of AD progression in which beta-amyloid pathology (as measured by CSF $A\beta_{1-42}$ or amyloid PET scan) appears first, followed by tau pathology (measured by CSF tau), then neuronal loss (measured by MRI) and then clinical symptoms (Jack et al., 2010; Jack et al., 2013). This model has received strong support over the years (Balsis et al., 2018; Broadhouse et al., 2021; Han and Shi, 2016; Jack et al., 2010; Nettiksimmons et al., 2014; van Rossum et al., 2012; Weiner et al., 2015; Yang et al., 2012; Yasuno et al., 2021), although not all findings align with it and alternative scenarios have emerged where beta-amyloid deposition, tau pathology, neuronal degeneration and cognitive loss aligned in a narrow time sequence (Braak et al., 2013; Edmonds et al., 2015b). Hence, through the prism of the amyloid cascade model, our MCI subgroups would rather represent distinct stages along the course of AD, the disease progressing from the amnestic stage to the mixed stage. However, the question of whether amnestic and mixed MCI subgroups merely reflect different stages along the course of AD or correspond to distinct MCI phenotypes could only receive a definite answer by examining longitudinal data from the 2 subgroups. This could hopefully be achieved in future research.

5. Limitations

It is important to note that data from the ADNI 1 were acquired from a 1.5 T scanner while data from the ADNI 2 were acquired from a 3 T scanner. It is an ongoing debate if scans acquired from different scanners can be merged. Many studies reported highly reproducible correspondence between volumes (Ho et al., 2010; Roche et al., 2013) while other studies suggested different methods to increase consistency across field strengths (Keihaninejad et al., 2010). Here, we have made the decision to preprocess all scans using the Combat harmonization method. Additionally, we assessed brain integrity from grey matter volume only, while other measures of structural integrity such as cortical thickness and diffusion in white matter would have been informative as well. Another limitation of our study includes the use of one dataset (i.e., ADNI). ADNI is not a population-based study and there are strict inclusion and exclusion criteria for selection of participants, which can affect generalizability of our findings. Therefore, validating our models and outcomes in other population-based studies and clinical trials would be an important next step. Future studies may also focus on different aspects of MCI subtyping. For example, socio-professional differences between MCI subgroups could be investigated as it can be relevant for finding risk factors. MCI clusters could also be derived from brain patterns and compared with clusters derived from cognitive scores. Regarding labeling of the MCI subgroups, we employed common terminology used in studies that have empirically derived subtypes of MCI. However, the amnestic subtype may also result from a host of non-AD pathologies, notably limbic-predominant age-related TDP-43 encephalopathy (LATE), which also manifests as a relatively circumscribed amnestic syndrome and targets the medial temporal lobe (Botha et al., 2018; Buciuc et al., 2020; Grothe et al., 2023). Finally, it is also important to mention that the MCI subtypes revealed in the present study reflect canonical extremes of a spectral representation of the MCI spectrum, and that a given MCI individual may not be perfectly represented by a given subtype and may express features of more than one subtype to varying extents.

6. Conclusion

In summary, our research revealed 3 latent subgroups underlying MCI participants of the ADNI database: an amnestic MCI, a mixed MCI and a cluster-derived normal subgroup. Leveraging on machine learning, our findings further suggest that MCI subtypes, extracted from a multidimensional neuropsychological approach, have proper biological and neurological characteristics. As such, multdimensional neuropsychological subtyping, in addition to being clinically meaningful, is also biologically and neurologically meaningful. Furthermore, our results suggested that AD progression may start by affecting memory and CSF biomarkers, followed by alterations in brain structure and other cognitive functions.

CRediT authorship contribution statement

JLB: Study concept, Plan of analysis, Data management, Image analysis, Statistical analysis, Literature search and review, Write-up of parts of the manuscript, Revision of the manuscript. **MN**: Study concept, Plan of analysis, Assistance with image and statistical analysis, Literature search and review, Revision of the manuscript. **ND**: Study concept, Plan of analysis, Assistance with image and statistical analysis, Revision of the manuscript. **LD**: Study concept, Plan of analysis, Assistance with statistical analysis, Literature search and review, Revision of the manuscript. **FC**: Study concept, Plan of analysis, Assistance with image and statistical analysis, Literature search and review, Write-up of parts of the manuscript, Revision of the manuscript.

Disclosure statement

The authors have no actual or potential conflicts of interest.

Acknowledgements

The study was funded by the CARSAT (Caisse Régionale d'Assurance Retraite et de la Santé au Travail) of Normandie (France) and from donations to the Caen Normandie Health Foundation (sponsors: Crédit Agricole Normandie and Normandie-Seine, Harmonie Mutuelle, SAMMed company), and co-funded by the European Union and the Normandie Region as part of the Operationnal FEDER program 2014-2020 Normandie. Data collection and sharing for this project was funded by the ADNI (National Institutes of Health Grant U01 AG024904) and DOD ADNI (Department of Defense award number W81XWH-12-2-0012). ADNI is funded by the National Institute on Aging, the National Institute of Biomedical Imaging and Bioengineering, and through generous contributions from the following: AbbVie, Alzheimer's Association; Alzheimer's Drug Discovery Foundation; Araclon Biotech; BioClinica, Inc.; Biogen; Bristol-Myers Squibb Company; CereSpir, Inc.; Cogstate; Eisai Inc.; Elan Pharmaceuticals, Inc.; Eli Lilly and Company; EuroImmun; F. Hoffmann-La Roche Ltd and its affiliated company Genentech, Inc.; Fujirebio; GE Healthcare; IXICO Ltd.; Janssen Alzheimer Immunotherapy Research & Development, LLC.; Johnson & Johnson Pharmaceutical Research & Development LLC.; Lumosity; Lundbeck; Merck & Co., Inc.; Meso Scale Diagnostics, LLC.; NeuroRx Research; Neurotrack Technologies; Novartis Pharmaceuticals Corporation; Pfizer Inc.; Piramal Imaging; Servier; Takeda Pharmaceutical Company; and Transition Therapeutics. The Canadian Institutes of Health Research is providing funds to support ADNI clinical sites in Canada. Private sector contributions are facilitated by the Foundation for the National Institutes of Health (www.fnih.org). The grantee organization is the Northern California Institute for Research and Education, and the study is coordinated by the Alzheimer's Therapeutic Research Institute at the University of Southern California. ADNI data are disseminated by the Laboratory for Neuro Imaging at the University of Southern California.

Verification

Our work has not been published previously, it is not under consideration for publication elsewhere, its publication is approved by all authors and tacitly or explicitly by the responsible authorities where the work was carried out, and if accepted, it will not be published elsewhere in the same form, in English or in any other language, including electronically without the written consent of the copyright holder.

Appendix A. Supporting material

Supplementary data associated with this article can be found in the online version at doi:10.1016/j.neurobiolaging.2023.07.006.

References

Alzheimer's Association, 2019. 2019 Alzheimer's disease facts and figures. Alzheimer's Dement. 15 (3), 321–387. https://doi.org/10.1016/j.jalz.2019.01.010

Anderson, Nicole D., 2019. State of the science on mild cognitive impairment (MCI). CNS Spectr. 24 (1), 78–87. https://doi.org/10.1017/S1092852918001347

Balsis, Steve, Geraci, Lisa, Benge, Jared, Lowe, Deborah A., Choudhury, Tabina K., Tirso, Robert, Doody, Rachelle S., Alzheimer's Disease Neuroimaging Initiative, 2018. Statistical model of dynamic markers of the Alzheimer's pathological cascade. J. Gerontol: Series B 73 (6), 964–973. https://doi.org/10.1093/geronb/gbx156

Bangen, Katherine J., Clark, Alexandra L., Werhane, Madeline, Edmonds, Emily C., Nation, Daniel A., Evangelista, Nicole, Libon, David J., Bondi, Mark W., Delano-

Wood, Lisa, 2016. Cortical amyloid burden differences across empirically-derived mild cognitive impairment subtypes and interaction with APOE E4 genotype. J. Alzheimer's Dis.: JAD 52 (3), 849–861. https://doi.org/10.3233/JAD-150900

Blanken, Anna E., Dutt, Shubir, Li, Yanrong, Nation, Daniel A., Alzheimer's Disease Neuroimaging Initiative, 2019. Disentangling heterogeneity in Alzheimer's disease: 2 empirically-derived subtypes. J. Alzheimer's Dis. 70 (1), 227–239.

Blanken, Anna E., Jang, Jung Yun, Ho, Jean K., Edmonds, Emily C., Han, S.Duke, Bangen, Katherine J., Nation, Daniel A., 2020. Distilling heterogeneity of mild cognitive impairment in the national Alzheimer's coordinating center database using latent profile analysis. JAMA Netw. Open 3 (3), e200413. https://doi.org/10.1001/jamanetworkopen.2020.0413

Bondi, Mark W., Edmonds, Emily C., Jak, Amy J., Clark, Lindsay R., Delano-Wood, Lisa, McDonald, Carrie R., Nation, Daniel A., Libon, David J., Au, Rhoda, Galasko, Douglas, 2014. Neuropsychological criteria for mild cognitive impairment improves diagnostic precision, biomarker associations, and progression rates. J. Alzheimer's Dis. 42 (1), 275–289.

Botha, H., Mantyh, W.G., Murray, M.E., Knopman, D.S., Przybelski, S.A., Wiste, H.J., Graff-Radford, J., Josephs, K.A., Schwarz, C.G., Kremers, W.K., Boeve, B.F., Petersen, R.C., Machulda, M.M., Parisi, J.E., Dickson, D.W., Lowe, V., Jack Jr, C.R., Jones, D.T., 2018. FDG-PET in tau-negative amnestic dementia resembles that of autopsy-proven hippocampal sclerosis. Brain 141 (4), 1201–1217. https://doi.org/10.1093/brain/awy049. PMID: 29538658; PMCID: PMC5889045.

Braak, H., Braak, E., 1991. Neuropathological stageing of Alzheimer-related changes. Acta Neuropathol. 82 (4), 239–259. https://doi.org/10.1007/BF00308809

Braak, Heiko, Zetterberg, Henrik, Del Tredici, Kelly, Blennow, Kaj, 2013. Intraneuronal tau aggregation precedes diffuse plaque deposition, but amyloid-β changes occur before increases of tau in cerebrospinal fluid. Acta Neuropathol. 126 (5), 631–641. https://doi.org/10.1007/s00401-013-1139-0

Broadhouse, Kathryn M., Winks, Natalie J., Summers, Mathew J., 2021. Fronto-temporal functional disconnection precedes hippocampal atrophy in clinically confirmed multi-domain amnestic mild cognitive impairment. EXCLI J. 20, 1458–1473. https://doi.org/10.17179/excli2021-4191

Buciuc, M., Botha, H., Murray, M.E., Schwarz, C.G., Senjem, M.L., Jones, D.T., Knopman, D.S., Boeve, B.F., Petersen, R.C., Jack Jr, C.R., Petrucelli, L., Parisi, J.E., Dickson, D.W., Lowe, V., Whitwell, J.L., Josephs, K.A., 2020. Utility of FDG-PET in diagnosis of Alzheimer-related TDP-43 proteinopathy. Neurology 95 (1), e23–e34. https://doi.org/10.1212/WNL.0000000000009722

Bzdok, Danilo, Engemann, Denis, Thirion, Bertrand, 2020. Inference and prediction diverge in biomedicine. Patterns 1 (8), 100119. https://doi.org/10.1016/j.patter.2020.100119

Bzdok, Danilo, Thomas Yeo, B.T., 2017. Inference in the age of big data: future perspectives on neuroscience. NeuroImage 155, 549–564. https://doi.org/10.1016/j.neuroimage.2017.04.061

Charrad, Malika, Ghazzali, Nadia, Boiteau, V.éronique, Niknafs, Azam, 2014. NbClust: an R package for determining the relevant number of clusters in a data set. J. Stat. Softw. 61, 1–36. https://doi.org/10.18637/jss.v061.i06

Chelune, Gordon J., Bornstein, Robert A., Prifitera, Aurelio, 1990. The Wechsler memory scale—revised. In: McReynolds, Paul, Rosen, James C., Chelune, Gordon J. (Eds.), Advances in Psychological Assessment: Volume 7. Springer US, Boston, MA, pp. 65–99. https://doi.org/10.1007/978-1-4613-0555-2_3

Clark, Lindsay R., Delano-Wood, Lisa, Libon, David J., McDonald, Carrie R., Nation, Daniel A., Bangen, Katherine J., Jak, Amy J., Au, Rhoda, Salmon, David P., Bondi, Mark W., 2013. Are empirically-derived subtypes of mild cognitive impairment consistent with conventional subtypes? J. Int. Neuropsychol. Soc. 19 (6), 635–645.

Dams-O'Connor, Kristen, Bellgowan, Patrick S.F., Corriveau, Roderick, Pugh, Mary Jo, Smith, Douglas H., Schneider, Julie A., Whitaker, Keith, Zetterberg, Henrik, 2021. Alzheimer's disease-related dementias summit 2019: national research priorities for the investigation of traumatic brain injury as a risk factor for Alzheimer's disease and related dementias. J. Neurotrauma 38 (23), 3186–3194. https://doi.org/10.1089/neu.2021.0216

Dickerson, Bradford C., Wolk, David A., 2011. Dysexecutive versus amnesic phenotypes of very mild Alzheimer's disease are associated with distinct clinical, genetic and cortical thinning characteristics. J. Neurol. Neurosurg. Psychiatry 82 (1), 45–51. https://doi.org/10.1136/jnnp.2009.199505

Edmonds, Emily C., Delano-Wood, Lisa, Clark, Lindsay R., Jak, Amy J., Nation, Daniel A., McDonald, Carrie R., Libon, David J., et al., 2015. Susceptibility of the conventional criteria for mild cognitive impairment to false-positive diagnostic errors. Alzheimer's Dement. 11 (4), 415–424. https://doi.org/10.1016/j.jalz.2014.03.005

Edmonds, Emily C., Delano-Wood, Lisa, Galasko, Douglas R., Salmon, David P., Bondi, Mark W., Alzheimer's Disease Neuroimaging Initiative, 2015. Subtle cognitive decline and biomarker staging in preclinical Alzheimer's disease. J. Alzheimer's Dis. 47 (1), 231–242. https://doi.org/10.3233/JAD-150128

Edmonds, Emily C., Eppig, Joel, Bondi, Mark W., Leyden, Kelly M., Goodwin, Bailey, Delano-Wood, Lisa, McDonald, Carrie R., Alzheimer's Disease Neuroimaging Initiative, 2016. Heterogeneous cortical atrophy patterns in MCI not captured by conventional diagnostic criteria. Neurology 87 (20), 2108–2116.

Edmonds, Emily C., McDonald, Carrie R., Marshall, Anisa, Thomas, Kelsey R., Eppig, Joel, Weigand, Alexandra J., Delano-Wood, Lisa, Galasko, Douglas R., Salmon, David P., Bondi, Mark W., 2019. Early versus late MCI: improved MCI staging using a neuropsychological approach. Alzheimer's Dement. 15 (5), 699–708.

Edmonds, Emily C., Smirnov, Denis S., Thomas, Kelsey R., Graves, Lisa V., Bangen, Katherine J., Delano-Wood, Lisa, Galasko, Douglas R., Salmon, David P., Bondi, Mark W., 2021. Data-driven versus consensus diagnosis of MCI: enhanced sensitivity for detection of clinical, biomarker, and neuropathologic outcomes. Neurology 97 (13), e1288–e1299. https://doi.org/10.1212/WNL.0000000000012600

Edmonds, Emily C., Weigand, Alexandra J., Hatton, Sean N., Marshall, Anisa J., Thomas, Kelsey R., Ayala, Daniela A., Bondi, Mark W., McDonald, Carrie R., 2020. Patterns of longitudinal cortical atrophy over 3 years in empirically derived MCI subtypes. Neurology 94 (24), e2532–e2544. https://doi.org/10.1212/WNL.0000000000009462

Efron, Bradley, 2010. Theoretical, permutation, and empirical null distributions. Large-Scale Inference: Empirical Bayes Methods for Estimation, Testing, and Prediction. Cambridge University Press, Cambridge, Institute of Mathematical Statistics Monographs, pp. 89–112. https://doi.org/10.1017/CBO9780511761362.007

Eppig, Joel S., Edmonds, Emily C., Campbell, Laura, Sanderson, Mark, Delano-Wood, Lisa, Bondi, Mark W., 2017. Statistically-derived subtypes and associations with cerebrospinal fluid and genetic biomarkers in mild cognitive impairment: a latent profile analysis. J. Int. Neuropsychol. Soc. 23 (7), 564–576. https://doi.org/10.1017/S135561771700039X

Fortin, J.-P., Sweeney, E.M., Muschelli, J., Crainiceanu, C.M., Shinohara, R.T., 2016. Removing inter-subject technical variability in magnetic resonance imaging studies. NeuroImage 132, 198–212.

Friston, Karl J., Holmes, Andrew P., Worsley, Keith J., Poline, J.-P., Frith, Chris D., Frackowiak, Richard S.J., 1994. Statistical parametric maps in functional imaging: a general linear approach. Hum. Brain Mapp. 2 (4), 189–210.

Ghosh, Sayantani, Libon, David, Lippa, Carol, 2014. Mild cognitive impairment: a brief review and suggested clinical algorithm. Am. J. Alzheimer's Dis. Other Dement. 29 (4), 293–302. https://doi.org/10.1177/1533317513517040

Grothe, M.J., Moscoso, A., Silva-Rodríguez, J., Lange, C., Nho, K., Saykin, A.J., Nelson, P.T., Schöll, M., Buchert, R., Teipel, S., 2023 Apr. Alzheimer's disease neuroimaging initiative. Differential diagnosis of amnestic dementia patients based on an FDG-PET signature of autopsy-confirmed LATE-NC. Alzheimers Dement. 19 (4), 1234–1244. https://doi.org/10.1002/alz.12763

Han, Pengcheng, Shi, Jiong, 2016. A theoretical analysis of the synergy of amyloid and tau in Alzheimer's disease. J. Alzheimer's Dis. 52 (4), 1461–1470. https://doi.org/10.3233/JAD-151206

Hansson, Oskar, Zetterberg, Henrik, Buchhave, Peder, Londos, Elisabet, Blennow, Kaj, Minthon, Lennart, 2006. Association between CSF biomarkers and incipient Alzheimer's disease in patients with mild cognitive impairment: a follow-up study. Lancet Neurol. 5 (3), 228–234. https://doi.org/10.1016/S1474-4422(06)70355-6

Hanyu, Haruo, Shimizu, Soichiro, Hirao, Kentaro, Kanetaka, Hidekazu, Sakurai, Hirofumi, Iwamoto, Toshihiko, Koizumi, Kiyoshi, Abe, Kimihiko, 2006. Differentiation of dementia with lewy bodies from Alzheimer's disease using mini-mental state examination and brain perfusion SPECT. J. Neurol. Sci. 250 (1), 97–102. https://doi.org/10.1016/j.jns.2006.07.007

Hastie, Trevor, Tibshirani, Robert, Friedman, Jerome H., 2009. Linear methods for classification. The Elements of Statistical Learning: Data Mining, Inference, and Prediction. Springer Series in Statistics Springer, New York, NY, pp. 101–137. https://doi.org/10.1007/978-0-387-84858-7

He, Jing, Farias, Sarah, Martinez, Oliver, Reed, Bruce, Mungas, Dan, DeCarli, Charles, 2009. Differences in brain volume, hippocampal volume, cerebrovascular risk factors, and apolipoprotein e4 among mild cognitive impairment subtypes. Arch. Neurol. 66 (11), 1393–1399. https://doi.org/10.1001/archneurol.2009.252

Ho, A.J., Hua, X., Lee, S., Leow, A.D., Yanovsky, I., Gutman, B., Dinov, I.D., Leporé, N., Stein, J.L., Toga, A.W., 2010. Comparing 3 T and 1.5 T MRI for tracking Alzheimer's disease progression with tensor-based morphometry. Hum. Brain Mapp. 31, 499–514.

Ingala, S., Tomassen, J., Collij, L.E., Prent, N., van 't Ent, D., Ten Kate, M., Konijnenberg, E., Yaqub, M., Scheltens, P., de Geus, E.J.C., Teunissen, C.E., Tijms, B., Wink, A.M., Barkhof, F., van Berckel, B.N.M., Visser, P.J., den Braber, A., 2021. Amyloid-driven disruption of default mode network connectivity in cognitively healthy individuals. Brain Commun. 3 (4), fcab201. https://doi.org/10.1093/braincomms/fcab201

Insel, Philip S., Hansson, Oskar, Mackin, R.Scott, Weiner, Michael, Mattsson, Niklas, 2018. Amyloid pathology in the progression to mild cognitive impairment. Neurobiol. Aging 64, 76–84. https://doi.org/10.1016/j.neurobiolaging.2017.12.018

Jack, Clifford R., Bennett, David A., Blennow, Kaj, Carrillo, Maria C., Feldman, Howard H., Frisoni, Giovanni B., Hampel, Harald, et al., 2016. A/T/N: an unbiased descriptive classification scheme for Alzheimer disease biomarkers. Neurology 87 (5), 539–547. https://doi.org/10.1212/WNL.0000000000002923

Jack Jr, Clifford R., Wiste, Heather J., Vemuri, Prashanthi, Weigand, Stephen D., Senjem, Matthew L., Zeng, Guang, Bernstein, Matt A., et al., 2010. Brain beta-amyloid measures and magnetic resonance imaging atrophy both predict time-to-progression from mild cognitive impairment to Alzheimer's disease. Brain 133 (11), 3336–3348. https://doi.org/10.1093/brain/awq277

Jack, Clifford R., Wiste, Heather J., Weigand, Stephen D., Knopman, David S., Lowe, Val, Vemuri, Prashanthi, Mielke, Michelle M., et al., 2013. Amyloid-first and neurodegeneration-first profiles characterize incident amyloid PET positivity. Neurology 81 (20), 1732–1740. https://doi.org/10.1212/01.wnl.0000435556.21319.e4

Jack Jr, Clifford R., Knopman, David S., Jagust, William J., Shaw, Leslie M., Aisen, Paul S., Weiner, Michael W., Petersen, Ronald C., Trojanowski, John Q., 2010. Hypothetical model of dynamic biomarkers of the Alzheimer's pathological cascade. Lancet Neurol. 9 (1), 119–128.

Jak, Amy J., Bondi, Mark W., Delano-Wood, Lisa, Wierenga, Christina, Corey-Bloom, Jody, Salmon, David P., Delis, Dean C., 2009. Quantification of 5 neuropsychological

approaches to defining mild cognitive impairment. Am. J. Geriatr. Psychiatry 17 (5), 368–375. https://doi.org/10.1097/JGP.0b013e31819431d5
Jessen, Frank, Wolfsgruber, Steffen, Wiese, Birgitt, Bickel, Horst, Mösch, Edelgard, Kaduszkiewicz, Hanna, Pentzek, Michael, et al., 2014. AD dementia risk in late MCI, in early MCI, and in subjective memory impairment. Alzheimer's Dement. 10 (1), 76–83. https://doi.org/10.1016/j.jalz.2012.09.017
Johnson, Julene K., Pa, Judy, Boxer, Adam L., Kramer, Joel H., Freeman, Katie, Yaffe, Kristine, 2010. Baseline predictors of clinical progression among patients with dysexecutive mild cognitive impairment. Dement. Geriatr. Cogn. Disord. 30 (4), 344–351. https://doi.org/10.1159/000318836
Johnson, W.E., Li, C., Rabinovic, A., 2007. Adjusting batch effects in microarray expression data using empirical Bayes methods. Biostatistics 8, 118–127.
Junquera Fernández, Almudena, García, Estefanía, Parra, Mario A., Fernández Guinea, Sara, 2020. Patterns of brain atrophy in dysexecutive amnestic mild cognitive impairment raise confidence about prodromal AD dementia. Alzheimer's Dement. 16 (S6), e046365. https://doi.org/10.1002/alz.046365
Kärkkäinen, Mikko, Prakash, Mithilesh, Zare, Marzieh, Tohka, Jussi, for the Alzheimer's Disease Neuroimaging Initiative, 2020. Structural brain imaging phenotypes of mild cognitive impairment (MCI) and Alzheimer's disease (AD) found by hierarchical clustering. Int. J. Alzheimer's Dis. 2020, 2142854. https://doi.org/10.1155/2020/2142854
Keihaninejad, S., Heckemann, R.A., Fagiolo, G., Symms, M.R., Hajnal, J.V., Hammers, A., Alzheimer's Disease Neuroimaging Initiative, 2010. A robust method to estimate the intracranial volume across MRI field strengths (1.5 T and 3T). Neuroimage 50, 1427–1437.
Kwak, Kichang, Giovanello, Kelly S., Bozoki, Andrea, Styner, Martin, Dayan, Eran, 2021. Subtyping of mild cognitive impairment using a deep learning model based on brain atrophy patterns. Cell Rep. Med. 2 (12), 100467. https://doi.org/10.1016/j.xcrm.2021.100467
Machulda, Mary M., Lundt, Emily S., Albertson, Sabrina M., Kremers, Walter K., Mielke, Michelle M., Knopman, David S., Bondi, Mark W., Petersen, Ronald C., 2019. Neuropsychological subtypes of incident mild cognitive impairment in the Mayo clinic study of aging. Alzheimer's Dement. 15 (7), 878–887. https://doi.org/10.1016/j.jalz.2019.03.014
Machulda, Mary M., Lundt, Emily S., Albertson, Sabrina M., Spychalla, Anthony J., Schwarz, Christopher G., Mielke, Michelle M., Jack Jr., Clifford R., et al., 2020. Cortical atrophy patterns of incident MCI subtypes in the Mayo clinic study of aging. Alzheimer's Dement. 16 (7), 1013–1022. https://doi.org/10.1002/alz.12108
Mattsson, Niklas, Zetterberg, Henrik, Hansson, Oskar, Andreasen, Niels, Parnetti, Lucilla, Jonsson, Michael, Herukka, Sanna-Kaisa, et al., 2009. CSF biomarkers and incipient Alzheimer disease in patients with mild cognitive impairment. JAMA 302 (4), 385–393. https://doi.org/10.1001/jama.2009.1064
Nettiksimmons, Jasmine, DeCarli, Charles, Landau, Susan, Beckett, Laurel, 2014. Biological heterogeneity in ADNI amnestic mild cognitive impairment. Alzheimer's Dement. 10 (5), 511–521.e1. https://doi.org/10.1016/j.jalz.2013.09.003
Nichols, Thomas E., Holmes, Andrew P., 2002. Nonparametric permutation tests for functional neuroimaging: a primer with examples. Hum. Brain Mapp. 15 (1), 1–25.
Ortega, Ricard L., Dakterzada, Farida, Arias, Alfonso, Blasco, Ester, Naudí, Alba, Garcia, Francisco P., Piñol-Ripoll, Gerard, 2019. Usefulness of CSF biomarkers in predicting the progression of amnesic and nonamnesic mild cognitive impairment to Alzheimer's disease. Curr. Aging Sci. 12 (1), 35–42. https://doi.org/10.2174/1874609812666190112095430
Overton, Marieclaire, Pihlsgård, Mats, Elmståhl, S.ölve, 2019. Diagnostic stability of mild cognitive impairment, and predictors of reversion to normal cognitive functioning. Dement. Geriatr. Cogn. Disord. 48 (5–6), 317–329.
Park, Jung Eun, Choi, Kyu Yeong, Kim, Byeong C., Choi, Seong-Min, Song, Min-Kyung, Lee, Jang Jae, Kim, Jahae, et al., 2019. Cerebrospinal fluid biomarkers for the diagnosis of prodromal Alzheimer's disease in amnestic mild cognitive impairment. Dement. Geriatr. Cogn. Disord. Extra 9 (1), 100–113. https://doi.org/10.1159/000496920
Park, Lovingly Quitania, Gross, Alden L., McLaren, Donald G., Pa, Judy, Johnson, Julene K., Mitchell, Meghan, Manly, Jennifer J., 2012. Confirmatory factor analysis of the ADNI neuropsychological battery. Brain Imaging Behav. 6 (4), 528–539.
Pedregosa, Fabian, Varoquaux, Gael, Gramfort, Alexandre, Michel, Vincent, Thirion, Bertrand, Grisel, Olivier, Blondel, Mathieu et al. 2011. "Scikit-Learn: machine learning in python". Machine learning in python, 6.
Prosser, Angus M.J., Tossici-Bolt, Livia, Kipps, Christopher M., 2017. Occipital lobe and posterior cingulate perfusion in the prediction of dementia with lewy body pathology in a clinical sample. Nucl. Med. Commun. 38 (12), 1029–1035.
Rey, Andŕe, 1958. L'examen Clinique En Psychologie. [The Clinical Examination in Psychology.]. L'examen Clinique En Psychologie. Presses Universitaries De France, Oxford, England.
Roche, F., Singh, B., Schaerer, J., Belaroussi, B., Gouttard, S., Istace, A., Yu, H.J., Fletcher, E., Bracoud, L., Pachai, C., 2013. Reproducibility of intracranial and hippocampal volume quantification at 1.5 T and 3T MRI: application to ADNI I. Alzheimers Dement 9, P271.
Rosen, Wilma G., Mohs, Richard C., Davis, Kenneth L., 1984. A new rating scale for Alzheimer's disease. Am. J. Psychiatry 141 (11), 1356–1364. https://doi.org/10.1176/ajp.141.11.1356
Rossum, Ineke A. van, Visser, Pieter Jelle, Knol, Dirk L., van der Flier, Wiesje M., Teunissen, Charlotte E., Barkhof, Frederik, Blankenstein, Marinus A., Scheltens, Philip, 2012. Injury markers but not amyloid markers are associated with rapid progression from mild cognitive impairment to dementia in Alzheimer's disease. J. Alzheimer's Dis. 29 (2), 319–327. https://doi.org/10.3233/JAD-2011-111694
Saboo, Krishnakant V., Hu, Chang, Varatharajah, Yogatheesan, Przybelski, Scott A., Reid, Robert I., Schwarz, Christopher G., Graff-Radford, Jonathan, et al., 2022. Deep learning identifies brain structures that predict cognition and explain heterogeneity in cognitive aging. NeuroImage 251, 119020. https://doi.org/10.1016/j.neuroimage.2022.119020
Scheff, S.W., Price, D.A., Ansari, M.A., Roberts, K.N., Schmitt, F.A., Ikonomovic, M.D., Mufson, E.J., 2015. Synaptic change in the posterior cingulate gyrus in the progression of Alzheimer's disease. J. Alzheimers Dis. 43 (3), 1073–1090. https://doi.org/10.3233/JAD-141518
Shaw, Leslie M., Vanderstichele, Hugo, Knapik-Czajka, Malgorzata, Clark, Christopher M., Aisen, Paul S., Petersen, Ronald C., Blennow, Kaj, et al., 2009. Cerebrospinal fluid biomarker signature in Alzheimer's disease neuroimaging initiative subjects. Ann. Neurol. 65 (4), 403–413. https://doi.org/10.1002/ana.21610
Slot, Rosalinde E.R., Sietske, A.M.Sikkes, Berkhof, Johannes, Brodaty, Henry, Buckley, Rachel, Cavedo, Enrica, Dardiotis, Efthimios, et al., 2019. Subjective cognitive decline and rates of incident Alzheimer's disease and non-Alzheimer's disease dementia. Alzheimer's Dement. 15 (3), 465–476. https://doi.org/10.1016/j.jalz.2018.10.003
Sun, Pan, Lou, Wutao, Liu, Jianghong, Shi, Lin, Li, Kuncheng, Wang, Defeng, Mok, Vincent C.T., Liang, Peipeng, 2019. Mapping the patterns of cortical thickness in single-and multiple-domain amnestic mild cognitive impairment patients: a pilot study. Aging 11 (22), 10000.
Tapiola, Tero, Alafuzoff, Irina, Herukka, Sanna-Kaisa, Parkkinen, Laura, Hartikainen, P.äivi, Soininen, Hilkka, Pirttilä, Tuula, 2009. Cerebrospinal fluid β-amyloid 42 and tau proteins as biomarkers of Alzheimer-type pathologic changes in the brain. Arch. Neurol. 66 (3), 382–389.
Thomas, Kelsey R., Edmonds, Emily C., Eppig, Joel S., Wong, Christina G., Weigand, Alexandra J., Bangen, Katherine J., Jak, Amy J., Delano-Wood, Lisa, Galasko, Douglas R., Salmon, David P., 2019. MCI-to-normal reversion using neuropsychological criteria in the Alzheimer's disease neuroimaging initiative. Alzheimer's Dement. 15 (10), 1322–1332.
Thomas, Kelsey R., Eppig, Joel S., Weigand, Alexandra J., Edmonds, Emily C., Wong, Christina G., Jak, Amy J., Delano-Wood, Lisa, et al., 2019. Artificially low mild cognitive impairment to normal reversion rate in the Alzheimer's disease neuroimaging initiative. Alzheimer's Dement. 15 (4), 561–569. https://doi.org/10.1016/j.jalz.2018.10.008
Weiner, Michael W., Veitch, Dallas P., Aisen, Paul S., Beckett, Laurel A., Cairns, Nigel J., Cedarbaum, Jesse, Donohue, Michael C., et al., 2015. Impact of the Alzheimer's disease neuroimaging initiative, 2004 to 2014. Alzheimer's Dement. 11 (7), 865–884. https://doi.org/10.1016/j.jalz.2015.04.005
Whitwell, Jennifer L., Petersen, Ronald C., Negash, Selamawit, Weigand, Stephen D., Kantarci, Kejal, Ivnik, Robert J., Knopman, David S., Boeve, Bradley F., Smith, Glenn E., Jack Jr., Clifford R., 2007. Patterns of atrophy differ among specific subtypes of mild cognitive impairment. Arch. Neurol. 64 (8), 1130–1138. https://doi.org/10.1001/archneur.64.8.1130
Winblad, Bengt, Amouyel, Philippe, Andrieu, Sandrine, Ballard, Clive, Brayne, Carol, Brodaty, Henry, Cedazo-Minguez, Angel, et al., 2016. Defeating Alzheimer's disease and other dementias: a priority for European science and society. Lancet Neurol. 15 (5), 455–532. https://doi.org/10.1016/S1474-4422(16)00062-4
Xue, Chen, Sun, Haiting, Yue, Yingying, Wang, Siyu, Qi, Wenzhang, Hu, Guanjie, Ge, Honglin, et al., 2021. Structural and functional disruption of salience network in distinguishing subjective cognitive decline and amnestic mild cognitive impairment. ACS Chem. Neurosci. 12 (8), 1384–1394. https://doi.org/10.1021/acschemneuro.1c00051
Yang, Huanqing, Xu, Hua, Li, Qingfeng, Jin, Yan, Jiang, Weixiong, Wang, Jinghua, Wu, Yina, Li, Wei, Yang, Cece, Li, Xia, 2019. Study of brain morphology change in Alzheimer's disease and amnestic mild cognitive impairment compared with normal controls. Gen. Psychiatry 32 (2), e100005. https://doi.org/10.1136/gpsych-2018-100005
Yang, Xianfeng, Tan, Ming Zhen, Qiu, Anqi, 2012. CSF and brain structural imaging markers of the Alzheimer's pathological cascade. PLOS ONE 7 (12), e47406. https://doi.org/10.1371/journal.pone.0047406
Yasuno, Fumihiko, Nakamura, Akinori, Kato, Takashi, Iwata, Kaori, Sakurai, Takashi, Arahata, Yutaka, Washimi, Yukihiko, Hattori, Hideyuki, Ito, Kengo, 2021. An evaluation of the amyloid cascade model using in vivo positron emission tomographic imaging. Psychogeriatrics 21 (1), 14–23. https://doi.org/10.1111/psyg.12589